

# Radical Graft Polymerization of Styrene Sulfonate on Poly(ethylene terephthalate) Films for ACL Applications: “Grafting From” and Chemical Characterization

M. Ciobanu,<sup>†</sup> A. Siove,<sup>†</sup> V. Gueguen,<sup>†</sup> L. J. Gamble,<sup>‡</sup> D. G. Castner,<sup>‡</sup> and V. Migonney<sup>\*,†</sup>

*Laboratoire de Biomatériaux et Polymères de Spécialité (LBPS/B2OA - UMR 7052), Institut Galilée, Université Paris 13, 93430 Villetaneuse, France, and National ESCA and Surface Analysis Center for Biomedical Problems, Departments of Bioengineering and Chemical Engineering, Box 351750, University of Washington, Seattle, Washington 98195-1750*

*Received September 20, 2005; Revised Manuscript Received January 26, 2006*

The purpose of this study is to develop a reliable method of functionalizing poly(ethylene terephthalate) with bioactive polymers to produce a “biointegrable” artificial anterior cruciate ligament. Radical graft polymerization of the sodium salt of styrene sulfonate (NaSS) onto poly(ethylene terephthalate) (PET) films was performed using the “grafting from” technique. Prior to the grafting, the surfaces of poly(ethylene terephthalate) films were activated by ozonation to generate peroxide and hydroperoxide reactive species on the PET film surfaces. The radical polymerization of NaSS was initiated by thermal decomposition of the hydroperoxides. The grafted PET surfaces were characterized by a toluidin blue colorimetric method, X-ray photoelectron spectroscopy, contact angle measurements, and atomic force microscopy. The influence of ozonation time, monomer concentration, and temperature on NaSS grafting ratios was examined. A total of 30 min of ozonation followed by grafting from a 15% NaSS solution at 70 °C for 90 min or more resulted in attachment of poly(NaSS) chains to the PET film surfaces.

## Introduction

Knee ligaments are commonly injured, especially for people participating in sports such as skiing or football. Injury of the anterior cruciate ligament (ACL), in particular, can sometimes result in termination of an athletes’ participation in competition. After an ACL tear, the best solutions for repair are either ligament replacement by a tendon autograft or reconstruction using an artificial ligament. Even with a patellar bone–tendon–bone autograft, which is widely reported as one of the best solutions, the recovery time for full function of the ACL can be long (6 months or more). For young and active people, reconstruction with an artificial ligament may provide the best therapeutic option.<sup>1–4</sup>

After an early period of enthusiasm and intensive clinical use of artificial ligaments, failures became too frequent, so their use decreased. To address this problem, efforts in the past 20 years to improve the quality of artificial ligaments and their biocompatibility have focused on the nature of the polymer, the techniques for knitting and weaving the fabrics, and the surgical gestures.<sup>5–7</sup>

Despite the progress in polymer science and advances in surgical techniques that have been made, “failures” of synthetic ACL are still high. Clinical studies showed that these failures are mainly due to abrasion of the fiber structure and weak tissue integration. Abrasion can be avoided by using new techniques for weaving and knitting the artificial ligament. Weak tissue integration is directly related to the foreign body response of the host to the poly(ethylene terephthalate) (PET) synthetic polymer. Therefore, the surface properties of the synthetic ACL

must be modified to achieve better “biointegration” with the host. In the majority of cases of synthetic ACL failure, the observed pathologic response was the development of immature collagen on the prosthesis leading to uncontrolled fibroblast cell response and the accumulation of an unstructured fibrous tissue.

Grafting of natural<sup>8,9</sup> or synthetic polymers<sup>9–15</sup> and/or of peptides onto implant surfaces (either polymeric or metallic) is an interesting way to improve the biocompatibility of the implant. The grafted molecules can play several roles such as adding biological properties and/or masking the synthetic origin of the substrate. A common approach to surface modification has been to modify the hydrophilic and/or hydrophobic properties of the synthetic surfaces. For example, polymer surfaces can be made hydrophobic by fluorination to prevent cell adhesion.<sup>16,17</sup> Another approach consists of introducing specific chemical groups by grafting. Surface grafting of vinyl monomers onto a polymer surface can be achieved after reactive species have been generated on the surface by methods such as plasma, corona, or ozone treatments.<sup>15,17–19</sup> The reactive species (peroxides, hydroperoxides, etc.) generated by these treatments will initiate radical polymerization of vinyl or acrylic monomers, resulting in polymer chains grafted to polymer or metal surfaces.

To develop a new generation of artificial ligaments for ACL reconstruction, we undertook the grafting of anionic polymers, such as poly(sodium styrene sulfonate) (pNaSS) or poly(methacrylic acid) (pMA), onto PET tissue surfaces activated by ozonation. These “bioactive” polymers are known to exhibit interesting biological properties such as modulation of protein conformation, cell proliferation, and bacteria adhesion,<sup>20–25</sup> which provide hope for an improved host response to these grafted PET fabrics.

In this paper, we present a strategy for grafting PET films as well as their characterization with X-ray photoelectron spectroscopy (XPS), a colorimetric method, contact angle measure-

\* To whom correspondence should be addressed. E-mail: vmig@galilee.univ-paris13.fr.

<sup>†</sup> Université Paris 13.

<sup>‡</sup> University of Washington.

ments, and atomic force microscopy (AFM). The purpose of this study is to develop a reliable method of functionalizing PET with bioactive polymers that will lead to a “biointegrable” artificial ACL.<sup>6–7</sup> The functionalization of PET fabrics and the biological properties will be presented in a future paper.

## Experimental Section

**Materials. Purification and Preparation of Samples.** The PET films samples were cut from a commercial PET film (1 mm thick, Weber Métaux) either as squares (10 × 10 mm) of 0.03 g or as disks (16 mm diameter) of 0.055 g. Prior to the grafting, PET films were washed for 15 min in tetrahydrofuran (THF) and then twice rinsed with bi-distilled water. The samples were dried under vacuum at 65 °C.

The sodium salt of styrene sulfonate (NaSS) (Fluka) was purified by recrystallization in a mixture of H<sub>2</sub>O/ethanol (90/10). Typically 20 g of NaSS were dissolved in 500 mL of the mixed solvent at 70 °C, then filtrated under vacuum and kept at 4 °C for 24 h. Recrystallized NaSS was then dried under vacuum at 50 °C and kept under argon atmosphere at 4 °C prior to the experiment.

**Ozonation.** Ozone was generated from flowing dried oxygen exposed to high voltage (OZONAIR). Optimal conditions of ozonation were found to be as follows: room temperature, 0.6 L min<sup>-1</sup> oxygen and 100 V. Under these conditions, it was assumed that the ozone concentration in aqueous solution can reach 3% (v/v). Six PET films samples were placed in 70 mL of bi-distilled water and exposed to the ozone flow for times varying from 2 to 240 min.

**Grafting.** PET surfaces films were grafted by a radical polymerization initiated by the surface peroxides generated during the ozonation step. To determine the optimal grafting conditions the following parameters were varied: ozonation time, polymerization time and monomer concentration. Graft polymerization of NaSS onto the PET films was carried out under an argon atmosphere. Immediately after the ozonation treatment each PET sample was placed in a glass reactor containing 3 mL of an NaSS aqueous solution with a concentration of 5 or 15% (v/v). The reaction was carried out at 65 or 70 °C for different times: 30, 60, 90, 120, 150, or 180 min. Then, the sample was removed and extensively washed with bi-distilled water for 1 h.

**Grafting Characterization. X-ray Photoelectron Spectroscopy.** All XPS data were acquired with a Surface Science Instruments S-probe spectrometer. This instrument has a monochromatized Al K $\alpha$  X-ray source, hemispherical analyzer, multichannel detector, and low-energy electron flood gun for charge neutralization. The X-ray spot size used for these experiments was approximately 800  $\mu$ m × 800  $\mu$ m in size. Pressure in the analytical chamber during spectral acquisition was less than 5 × 10<sup>-9</sup> Torr. For elemental composition determination, spectra were acquired at an analyzer pass energy of 150 eV. The high-resolution C1s spectra were acquired at an analyzer pass energy of 50 eV. The takeoff angle (the angle between the sample normal and the input axis of the energy analyzer) for all XPS experiments was 55°. This takeoff angle corresponds to a sampling depth of approximately 5 nm. One or two spots on one or two replicates were analyzed for each sample treatment.

The Service Physics ESCAVB Graphics Viewer program was used to determine peak areas, calculate the elemental compositions from those peak areas, and peak fit the high-resolution spectra. Carbon, oxygen, and silicon concentrations were calculated from the C1s, O1s, and Si2p lines in 0–1000 eV survey scans. Sulfur and sodium concentrations were calculated from 20 eV scans centered around the S2p and Na1s lines. The binding energy scale was calibrated by assigning the hydrocarbon peak in the C1s high-resolution spectra to a binding energy of 285.0 eV. A Gaussian line shape was used to peak-fit the C1s high-resolution spectra.

**Toluidin Blue: Colorimetric Method.** The colorimetric method described by Ikada et al.<sup>9</sup> was adapted to the system. The protocol was the following: 50 mL of a 5 × 10<sup>-4</sup> M toluidine blue (TB) aqueous solution was prepared, and 0.2 mL of a buffer solution of 2-amino

**Table 1.** Superficial Tensions of Liquids Used for Surface Energy Calculation

liquid	$\gamma_L$ (mN m)	$\gamma_L^P$ (mN m)	$\gamma_L^D$ (mN m)
water	72.3	53.6	18.7
ethylene glycol	47.5	18.2	29.3
formamide	59	19.6	39.4
diiodomethane	50.8	1.3	49.5

2-methyl propanol was added to reach and maintain the solution pH value at 10. Each ozonated or ozonated plus NaSS grafted PET sample was placed in 6 mL of the TB solution at 30 °C for 6 h. Noncomplexed TB molecules were removed by rapid washing (30 min) of the sample with a basic aqueous solution (NaOH 5 × 10<sup>-4</sup>M, pH 9). Then, each sample was placed in 5–15 mL of an aqueous acetic acid solution (50%) (v/v) for 24 h to obtain complete de-complexation of TB from the sample.

The de-complexation solution was analyzed by UV/visible spectroscopy. Toluidin blue has an absorption peak at 633 nm, with an extinction coefficient of 50 000 L mol<sup>-1</sup> cm<sup>-1</sup>. It was assumed on the grafted surfaces that a 1/1 complex is formed between one TB molecule and one SO<sub>3</sub><sup>-</sup> group. Therefore, the grafting ratio (GR) was calculated as follows:

$$\text{GR (g of grafted polymer/cm}^2 \text{ film)} = CVM/2$$

where  $C$  = molar concentration of the monomer (mol L<sup>-1</sup>),  $V$  = acetic acid volume (L),  $M$  = molar weight of the monomer ( $M_{\text{NaSS}} = 206$  g mol<sup>-1</sup>)

**Contact Angle and Surface Energy.** Contact angle measurements were performed on a DSA 10 Kruss Instrument, using the sessile drop method. The volume of the liquid droplets was 0.5  $\mu$ L, and the contact angle determination for each sample was the average value of nine measurements on different parts of the film. The contact angles were measured with four liquid solvents (water, ethylene glycol, formamide, and diiodomethane). The tangent1 method of the software (DSA 1 Drop Shape Analysis) was chosen to measure the contact angle with a linear baseline, and the Owens–Wendt equation was applied to calculate the surface energy, including its polar and dispersive components. Values of liquids surface energies are shown in Table 1.

### Owens-Wendt Equation

$$\frac{\gamma_L(\cos \theta + 1)}{2(\gamma_L^D)^{1/2}} = (\gamma_S^P)^{1/2} \frac{(\gamma_L^P)^{1/2}}{(\gamma_L^D)^{1/2}} + (\gamma_S^P)^{1/2}$$

**Atomic Force Microscopy.** All AFM images were acquired using a Dimension 3100 (Digital Instruments Inc.) system. The tapping mode in air at the cantilever's resonant frequency was employed using a silicon probe and cantilever unit (resonance frequency 285 kHz). The scan rate was 1 Hz. The roughness parameter is the arithmetic average of the absolute values of the surface height deviations measurements from the mean plane:  $Ra = (1/n) \sum_{j=1}^n |Z_j|$

## Results and Discussion

**Influence of Ozonation Time.** The length of ozonation time and its influence on the active species concentration was studied. Six PET film samples were ozonated for 2, 5, 10, 20, 30, 60, and 240 min and then complexed with TB. It was assumed that oxidized species such as peroxides or hydroperoxides would form adsorption complexes with the TB molecules. Results were expressed in mol of TB per cm<sup>2</sup> of ozonated PET film versus time and are shown in Figure 1. These results showed a linear variation of TB adsorption with ozonation time: as ozonation time increases, the amount of TB complexed increases. This increase in TB complexation indicates that the amount of active surface species (peroxides, hydroperoxides, etc.) increases with

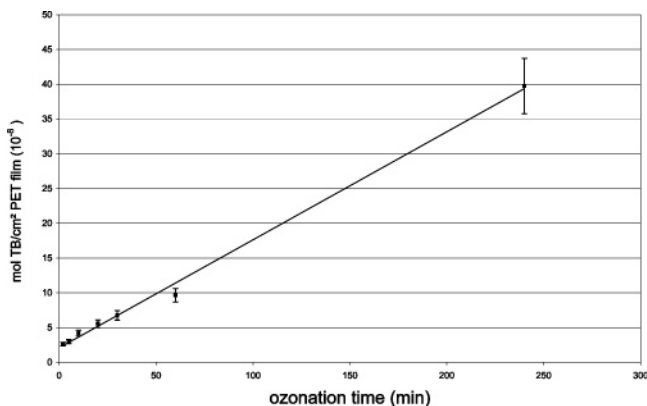


**Figure 1.** Adsorption of Toluidin Blue on PET film surfaces after ozonation.

**Table 2.** Liquid Contact Angles on Virgin and Ozonated PET Films

sample	contact angle (°)			
	water	ethylene glycol	formamide	diiodomethane
PET film	67 ± 3.3	49.5 ± 1.5	38.6 ± 2.3	39 ± 2.5
PET film ozonated 30 min	60.6 ± 4.3	47.5 ± 2.2	44.5 ± 2.9	45.9 ± 2.5
PET film ozonated 60 min	57.8 ± 3.4	43.7 ± 2.1	42.3 ± 2.4	46.7 ± 2.7
PET film ozonated 120 min	51 ± 5.2	51.6 ± 2.3	41.9 ± 2.7	49.7 ± 3.4
PET film ozonated 240 min	54 ± 5.3	40.7 ± 1.9	40.3 ± 2.6	51.6 ± 4.4

**Table 3.** Surface Energies of Virgin and Ozonated PET Films

surface	$\gamma_s$ (mN m)	$\gamma_s^p$ (mN m)	$\gamma_s^d$ (mN m)	polar part % $\frac{\gamma_s^p}{\gamma_s}$
virgin PET	42.2	11.6	30.8	37.6
PET film ozonated 30 min	42.6	18.1	24.5	73.8
PET film ozonated 60 min	44.0	20.0	24.0	83.3
PET film ozonated 120 min	47.6	26.0	21.6	123.8
PET film ozonated 240 min	44.7	24.4	20.3	120.2

ozonation time. However, it is also possible that at long ozonation times the macromolecular chains of PET could be altered or degraded, which would adversely affect the PET film properties. For this reason, the optimal time of ozonation was chosen to be 60 min.

**Contact Angle Results.** The results from contact angles measurements with the four liquids are shown in Table 2. Water contact angles decreased slightly with increasing ozonation time, showing that ozonation increases the hydrophilic nature of the PET film. The largest change in the water contact angle occurred

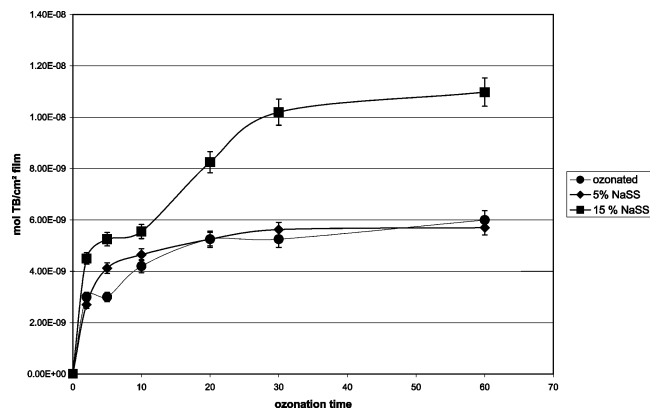


**Figure 2.** Toluidin blue absorbance on ozonated and grafted (5% and 15%) PET films.

in the first 30 min of ozonation. Beyond 60 min of ozonation the water contact angle remained relatively constant.

Surface energies, with their polar and dispersive components, were calculated by the Owens–Wendt method and are presented in Table 3. Results show that the surface energies of the films only increase slightly with ozonation time, whereas the polar part of the surface energy increased strongly. This observation is consistent with the ozonation treatment generating more polar species (e.g., hydroperoxides) at the PET surface.

**X-ray Photoelectron Spectroscopy.** The results from the XPS elemental compositional analysis for the untreated and treated PET film samples are summarized in Table 4. The theoretical XPS values expected for PET and NaSS, based on their stoichiometry, are also included in Table 4 for comparison. The untreated PET surface showed slightly more carbon than expected theoretically. This is typical for PET and is probably due to the adsorption of a small amount of adventitious hydrocarbon layer onto the PET surface. Ozone treatment of the surface did not significantly change surface composition of the PET films. The reason no significant differences were detected by XPS for these samples was that (1) the ozone treatment conditions were rather mild and (2) the species produced by ozonation are reactive. Thus, by the time the ozonated surfaces were analyzed by XPS (several days), they had probably converted back to a state similar to untreated PET.

**Influence of Monomer Concentration.** Six films of PET were ozonated for 2, 5, 10, 30, and 60 min. Then, they were grafted by radical polymerization of NaSS monomer for 90 min, according to the protocol described above. The monomer concentration was either 5 or 15% of NaSS/H<sub>2</sub>O (w/v). The temperature of the polymerization was 65 °C. Toluidin blue absorbance onto ozonated and grafted films are plotted against ozonation time in Figure 2. These results show that a critical

**Table 4.** XPS Determined Elemental Compositions of Virgin, Ozonated (30 and 60 min), and Ozonated Plus NaSS Grafted (30 min Ozone Plus Grafting for 30, 60, and 180 min) PET Films<sup>a</sup>

sample type	XPS atomic percent					
	carbon	oxygen	sodium	sulfur	silicon	other
PET (theory)	71.4	28.6				
virgin PET	74.6 ± 0.5	25.4 ± 0.5				
PET ozonated 30 min	74.8 ± 0.6	25.0 ± 0.3		trace	trace	
PET ozonated 60 min	74.5 ± 0.8	25.3 ± 0.4			trace	
PET ozonated 30 min + 30 min NaSS grafting	73.6 ± 1.0	24.2 ± 0.5	0.2 ± 0.1	0.2 ± 0.1	1.7 ± 0.2	trace F
PET ozonated 30 min + 60 min NaSS grafting	73.2 ± 0.2	23.5 ± 0.6	0.3 ± 0.1	0.3 ± 0.1	2.2 ± 0.4	trace F
PET ozonated 30 min + 180 min NaSS grafting	69.4 ± 5.2	22.9 ± 2.7	2.8 ± 1.3	3.5 ± 1.3	1.4 ± 0.1	trace F and N
NaSS (theory)	61.5	23.1	7.7	7.7		

<sup>a</sup> The XPS elemental compositions expected based on the stoichiometry of PET and NaSS are also included for comparison. Values are reported as averages ± one standard deviation. Trace means approximately 0.5 atomic percent or less of the element detected on one replicate.



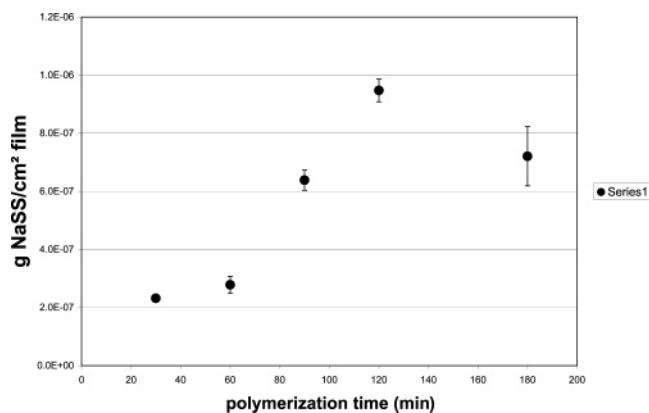


**Figure 3.** NaSS grafting ratio versus grafting time.  $T = 70\text{ }^{\circ}\text{C}$ , ozonation time = 30 min.

value of monomer concentration is needed to observe and measure NaSS grafting. As seen in Figure 2, when films are polymerized with 5% NaSS solutions, the TB absorbance is identical to that of the films that were only ozonated. In contrast, when films are polymerized with 15% NaSS solutions the increase in TB is significantly higher than that of the ozonated film. Therefore, the grafting ratios (GR) were calculated by the difference between the obtained TB values for the 15% NaSS polymerized films and those for the ozonated films. For example, after 60 min of ozonation, GR is  $1.1 \times 10^{-8} - 6 \times 10^{-9} = 5 \times 10^{-9}$  mol TB/cm<sup>2</sup> film. This corresponds to a GR of  $1 \times 10^{-6}$  g NaSS/cm<sup>2</sup> film. This value is consistent with the grafting of acrylic acid on PET described by Gupta<sup>11</sup> and Ikada.<sup>17</sup> Moreover, the results in Figure 2 show that the maximum grafting ratio is approached after 30 min of ozonation. Thus, an ozonation time of 30 min was selected for the next set of grafting experiments.

**Kinetics of Poly(NaSS) Grafting.** The extent of poly(NaSS) grafting with a 15% NaSS/H<sub>2</sub>O (w/v) solution after 30 min of ozonation, at 70 °C was determined at different polymerization times. The polymer grafting was characterized by TB complexation, chemical composition (XPS), topography (AFM), and surface energy (contact angles).

**Toluidin Blue Method.** The variation of the NaSS GR values versus the polymerization time is not linear as seen in Figure 3. Indeed, the GR values after 30 and 60 min of polymerization are approximately the same, 0.2–0.3  $\mu\text{g}$  NaSS/cm<sup>2</sup> of PET film whereas for polymerization time of 90, 120, to 180 min, the GR increased significantly to values of 0.6–0.9  $\mu\text{g}/\text{cm}^2$  then decrease to about 0.7  $\mu\text{g}/\text{cm}^2$ .

**X-ray Photoelectron Spectroscopy.** After ozonation and NaSS grafting the carbon and oxygen concentrations decreased while the sulfur and sodium concentrations increased, as expected based on the theoretical compositions of PET and NaSS (see Table 4). Only small changes in the XPS composition were observed after 30 and 60 min of NaSS grafting, consistent with the TB results. However, after 180 min of NaSS grafting, significantly larger changes in the XPS composition were observed. The grafting of NaSS onto the PET film surface should result in equal amounts of sodium and sulfur detected by XPS. Within the experimental error, this was true for all three NaSS grafted samples. Note that the XPS standard deviations increased significantly for the 180 min grafted sample. Variations in composition both from spot-to-spot on a replicate and from replicate-to-replicate were responsible for the increase in standard deviations. There was also a small amount of silicon detected on the NaSS grafted surfaces. The presence of silicon is probably due to introduction of small

**Table 5.** XPS High-Resolution C1s Results for Virgin, Ozonated (30 and 60 min), and Ozonated Plus NaSS Grafted (30 min Ozone Plus Grafting for 30, 60, and 180 min) PET Films<sup>a</sup>

sample type	XPS C1s Percent			shake-up satellite
	C–C/ C–H	C–O/ C–SO <sub>3</sub>	O–C=O	
PET (theory)	60	20	20	
virgin PET	63 ± 3	19 ± 2	16 ± 1	3 ± 1
PET ozonated 30 min	65 ± 1	18 ± 1	16 ± 1	2 ± 1
PET ozonated 60 min	64 ± 2	19 ± 1	16 ± 1	2 ± 1
PET ozonated 30 min + 30 min NaSS grafting	68 ± 1	16 ± 1	15 ± 1	2 ± 1
PET ozonated 30 min + 60 min NaSS grafting	67 ± 1	16 ± 1	15 ± 1	2 ± 1
PET ozonated 30 min + 60 min NaSS grafting	72 ± 5	14 ± 2	12 ± 2	2 ± 1
NaSS (theory)	87.5	12.5		

<sup>a</sup> The XPS carbon species expected based on the stoichiometry of PET and NaSS are also included in the table for comparison. Values are reported as averages ± one standard deviation.

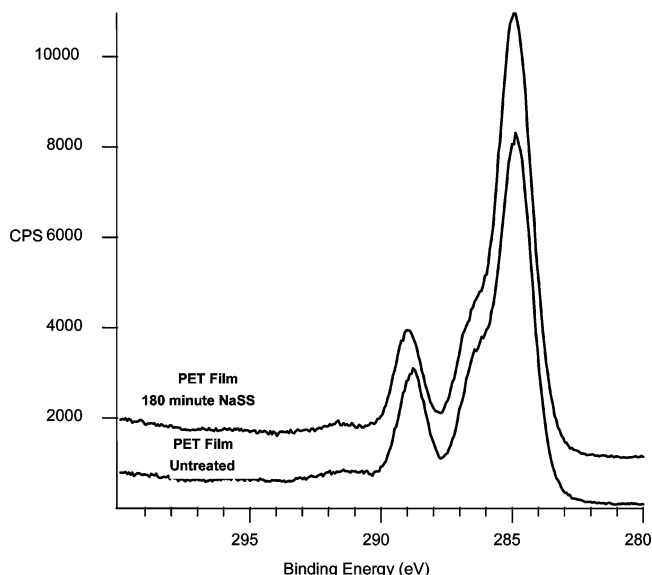


**Figure 4.** Representative XPS high-resolution C1s spectra acquired from untreated and 30m ozone plus 180m NaSS grafted PET films. The introduction of the NaSS groups from the grafting process result in an increase in the C–C/C–H species at 285 eV and a decrease in the C–O and O–C=O species at 287 and 289 eV, respectively.

amounts of poly(dimethyl siloxane) (PDMS) contamination onto the PET surface during the grafting process. The XPS composition of pure PDMS is 25% Si, 25% O, and 50% C.

The results from the analysis of the XPS high-resolution C1s spectra are summarized in Table 5. Also included in Table 5 are the expected amount of each carbon species, based on the stoichiometry of PET and NaSS. The results in Table 5 are consistent with the XPS compositional results discussed in the previous paragraph. No significant difference is observed between the untreated PET film surface and the PET films ozonated for 30 or 60 min. The amount of the C–C/C–H species detected at 285 eV in the untreated and ozonated films is slightly higher than expected from the stoichiometry of PET, consistent with the composition results in Table 3. After 30 min ozonation followed by 180 min of NaSS grafting, a significant increase in the amount of C–C/C–H species along with significant decreases in the amounts of C–O and O–C=O species were detected, as shown in Table 5 and Figure 4. This is expected due to the increased amount of C–C/C–H species in NaSS relative to PET.

**Contact Angle Results.** The results show that the poly(NaSS) grafting of the PET surface increases the hydrophilicity of the

**Table 6.** Liquid Contact Angles on Virgin and Grafted PET Film (30 min Ozonation, 1 h Grafting)

sample	contact angle (°)			
	water	ethylene glycol	formamide	diiodomethane
PET film	67.0 ± 3.3	49.5 ± 1.5	38.6 ± 2.3	39 ± 2.5
NaSS grafted PET film	57.0 ± 1.9	43.0 ± 2.6	48.1 ± 3.3	47.6 ± 3.6

**Table 7.** Surface Energies of Virgin and Grafted PET Film (30 min Ozonation, 1 h Grafting)

surface	$\gamma_s$ (mN m)	$\gamma_s^P$ (mN m)	$\gamma_s^D$ (mN m)	polar part % $\gamma_s^P/\gamma_s^D$
virgin PET	42.2	11.6	30.8	37.6
NaSS grafted PET film	44.3	21.9	22.4	97.8

**Table 8.** Roughness Parameters ( $R_a$ ) of Virgin, Ozonated, and Grafted Surfaces of PET

sample	$R_a$ (nm)
virgin PET	2.7 ± 0.2
ozonated PET	9.5 ± 2.6
1 h NaSS grafted PET	4.6 ± 0.5
3 h NaSS grafted PET	6.4 ± 0.4

surface. This is illustrated by the decrease of the water contact angle, from 67 to 57°, as shown in Table 6. Moreover, it is worthy to note that, although the grafted film surface energy is slightly higher, the polar percentage of the surface energy is increased by a factor of 3 (see Table 6). This increase in the polar contribution could be an important change with respect to the behavior of these films when they are in contact with biological species such as proteins and cells.

**AFM Observations.** The surface topography of PET films was measured by AFM before and after the grafting. Roughness parameters are reported in Table 8. Results show that the untreated film exhibits a smoother surface than the ozonated and grafted ones. Representative images of the PET film surface before and after grafting are shown in Figure 5.

## Conclusion

The purpose of this paper was to present the strategy for grafting a bioactive polymer onto PET that can be applied to PET fibers and fabrics used for artificial ligaments. The biologic properties exhibited by macromolecular chains bearing anionic groups such as sulfonate and carboxylate led us to choose the grafting of poly(sodium styrene sulfonate) and then optimize a protocol of grafting of this polymer onto PET.

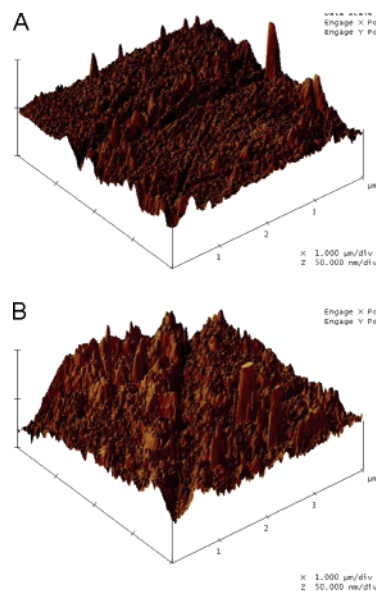
The results from the current study on PET films show the optimal conditions of grafting are as follows:

(1) The optimal ozonation times are between 30 and 60 min, allowing the formation sufficient quantities of active species such as peroxides and hydroperoxydes while preventing the degradation of the PET macromolecular chains.

(2) The concentration of the monomer in water must be 15% (w/v) to generate measurable grafted amounts of poly(NaSS).

(3) The grafting of poly(NaSS) was determined by both the Toluidin Blue colorimetric method and XPS. The results from both methods are in good agreement.

(4) Contact angle measurements show an increase in the hydrophilic properties of the modified PET films, as expected from grafting a hydrophilic polymer such poly(NaSS). The polar

**Figure 5.** AFM images of PET untreated (A) and 30 min ozonated + 180 min NaSS grafted PET (B).

component of the surface component also increased with grafting of poly(NaSS).

(5) The AFM observations show that ozonation and grafting of poly(NaSS) increases the roughness of the PET films.

The results provide a reliable method of functionalizing poly(ethylene terephthalate) with bioactive polymers. The functionalization of PET fabrics and the observed biological properties will be the subject of a future study.

**Acknowledgment.** The authors thank Bernard Brulez for his helpful contribution and the Lars Society (Arc sur Tille, France) for the financial support of the work. The XPS experiments were done at NESAC/BIO, which is supported by a grant from the National Institute of Biomedical Imaging and Bioengineering (EB-002027). The authors would also like to thank David Billet, from LPMTM (Université Paris 13), for AFM analysis.

## References and Notes

- (1) Cerulli, G.; Benoit, D. L.; Lamontagne, M.; Caraffa, A.; Liti, A. *Knee Surg. Sports Traumatol. Arthrosc.* **2003**, *11*, 307–311.
- (2) Fu, F. H.; Bennett, C. H.; Lattermann, C.; Ma, C. B. *Am. J. Sports Med.* **1999**, *27*, 821–830.
- (3) Fu, F. H.; Bennett, C. H.; Ma, C. B.; Menetrey, J.; Lattermann, C. *Am. J. Sports Med.* **2000**, *28*, 124–130.
- (4) Lavoie, P.; Fletcher, J.; Duval, N. *Knee* **2000**, *7*, 157–163.
- (5) Laboureaud, J. P.; Brulez, French Patent No. 2755846/58/21, 1998.
- (6) Migonney, V.; Pavon-Djavid, G.; Siove, A.; Ciobanu, M.; Brulez, French Patent No. 0300497, 2003.
- (7) Siove, A.; Pavon-Djavid, G.; Ciobanu, M.; Brulez, B.; Migonney, V. French Patent No. 0300495, 2003.
- (8) Bisson, I.; Kosinski, M.; Ruault, S.; Gupta, B.; Hilborn, J.; Wurm, F.; Frey, P. *Biomaterials* **2002**, *23*, 3149–3158.
- (9) Sano, S.; Kato, K.; Ikada, Y. *Biomaterials* **1993**, *14*, 817–822.
- (10) Crémieux, A.; Pavon-Djavid, G.; Saleh Mghir, A.; Hélar, G.; Migonney, V. *J. Appl. Biomater. Biomech.* **2003**, *1*, 178–185.
- (11) Gupta, B.; Hilborn, J. G.; Bisson, I.; Frey, P. *J. Appl. Polym. Sci.* **2001**, *81*, 2993–3001.
- (12) Gupta, B.; Plummer, C.; Bisson, I.; Frey, P.; Hilborn, J. *Biomaterials* **2002**, *23*, 863–871.
- (13) Kato, K.; Sano, S.; Ikada, Y. *Colloids Surf. B: Biointerfaces* **1995**, *4*, 221–230.
- (14) Park, S.; Bearinger, J. P.; Lautenschlager, E. P.; Castner, D. G.; Healy, K. E. *J. Biomed. Mater. Res.* **2000**, *53*, 568–576.
- (15) Sugiyama, K.; Kato, K.; Kido, M.; Shiraishi, K.; Ohga, K.; Okada, K.; Matsuo, O. *Macromol. Chem. Phys.* **1998**, *199*, 1201–1208.
- (16) Kato, K.; Ikada, Y. *Biotechnol. Bioeng.* **1995**, *47*, 557–566.

- (17) Kowalczyńska, H. M.; Nowak-Wyrzykowska, M. *Cell Biol. Int.* **2003**, 27, 101–114.
- (18) Ratner, B. D. *Biosens. Bioelectron.* **1995**, 10, 797–804.
- (19) Yuhai, G.; Jianchun, Z.; Meiwu, S. *J. Appl. Polym. Sci.* **1999**, 73, 1161–1164.
- (20) Berlot, S.; Aissaoui, Z.; Pavon-Djavid, G.; Belleney, J.; Jozefowicz, M.; Helary, G.; Migonney, V. *Biomacromolecules* **2002**, 3, 63–68.
- (21) El Khadali, F.; Helary, G.; Pavon-Djavid, G.; Migonney, V. *Biomacromolecules* **2002**, 3, 51–56.
- (22) Imbert-Laurenceau, E.; Berger, M.-C.; Pavon-Djavid, G.; Jouan, A.; Migonney, V. *Polymer* **2005**, 46, 1277–1285.
- (23) Latz, C.; Pavon-Djavid, G.; Helary, G.; Evans, M.; Migonney, V. *Biomacromolecules* **2003**, 4, 766–771.
- (24) Le Guillou-Buffello, D.; Helary, G.; Gindre, M.; Pavon-Djavid, G.; Laugier, P.; Migonney, V. *Biomaterials* **2005**, 26, 4197–4205.
- (25) Pavon-Djavid, G.; Helary, G.; Migonney, V. *ITBM-RBM* **2005**, 26, 183.

BM050694+